Sports Eng
DOI 10.1007/s12283-017-0239-9

ORIGINAL ARTICLE

A computational approach for predicting plant canopy induced wind effects on the trajectory of golf shots

Neda Yaghoobian[1,2] · **Rajat Mittal**[1]

Abstract Large-eddy simulation of atmospheric flow is combined with golf ball trajectory modeling that incorporates local plant canopy information to predict the trajectory of a golf shot at any hole on a golf course in a variety of wind conditions. The model is applied to examine golf shots on hole 12 of the Augusta National Golf Club, which is particularly well known for its wind-induced difficulty. The results indicate that the tree canopies around this hole play a significant role in golf ball trajectories and also induce a strong directional sensitivity on the landing spot of the ball for this hole.

Keywords Golf ball trajectory · Large-eddy simulation · Plant canopy · Wind effect

1 Introduction

Among all the environmental factors that affect the accuracy of golf shots, wind is, perhaps, the most important. The direction and strength of the wind alters the aerodynamic forces on a ball in flight, and consequently its speed, distance, and direction of travel. The fact that local wind conditions on any particular hole in a golf course change over time-scales ranging from a few seconds and minutes, to hours and days, introduces an element of variability in the ball trajectory that is not completely understood. Any such analysis is complicated by the effect of the local terrestrial and vegetation topology, as well as the inherent complexity of golf ball aerodynamics. In addition to the scientific challenge inherent in predicting this wind-induced variability on golf shots, any tools that can be developed to predict this variability could serve as an aid to competitive golfers, and could enrich the discussion and technical analysis of golf. Finally, sports such as golf represent a fertile medium for introducing state-of-the-art computational modeling techniques and principles of flow physics to the general public, and in doing so provide an opportunity to enhance the interest and support for scientific inquiry, in general, and for fluid dynamics in particular.

In the current study, we develop a computational framework for modeling and assessing the trajectory and accuracy of golf shots in the presence of wind- and hole-specific terrestrial topology and local plant canopy. The key components of the model are a large-eddy simulation (LES)-based approach for modeling the airflow over a golf hole that incorporates geo-specific information, and an accurate, dynamical model of a golf ball that is suitable for predicting the trajectory of a golf shot in complex wind conditions. While the two primary components of the modeling framework (modeling of local wind conditions and modeling of golf ball trajectory) are based on existing work, the contribution of the current work lies in the coupling of the two components in a manner appropriate for this analysis, and the application of the resulting method to examine golf shot variability at the 12th hole at the Augusta National Golf Club, an iconic hole in golf that is renowned for its wind-induced difficulty. It is noted that the methodology developed here could in-principle be

✉ Neda Yaghoobian
nyaghoo2@jhu.edu; nyaghoobian@fsu.edu

Rajat Mittal
mittal@jhu.edu

1 Department of Mechanical Engineering, Johns Hopkins University, Baltimore, MD, USA

2 Present Address: Department of Mechanical Engineering, Florida State University, Tallahassee, FL, USA

Published online: 02 June 2017

applied to any golf course/hole and overall approach could also be extended to other sports such as soccer, baseball, cricket, tennis, and American football, where aerodynamic forces play an important role in modifying the trajectory of the ball.

The paper is organized as follows: in Sect. 2, we describe some features of the 12th hole at the Augusta National Golf Club that are relevant to the current study. In Sect. 3, we present the key components of the computational methodology, which include the modeling of airflow over the golf hole and the dynamical modeling of the golf ball trajectory. In Sect. 4, we describe the results from our computational modeling and analysis of golf shots on this hole, and summary and conclusions are provided in Sect. 5.

2 Hole 12 at the Augusta National Golf Club

The Masters Golf Tournament is one of the four major championships in professional golf, and is played each year during the first week or second week of April at the Augusta National Golf Club, in Augusta, Georgia, USA (Fig. 1a). Hole 12 at this course (Fig. 1b), also named 'Golden Bell', is described as one of the most difficult par-3 holes in all the major golf championships [1, 2] with an all-time scoring average of 3.28 [3]. The green for this hole itself is narrow (9–13 m wide), thereby presenting a small target for golf shots. This small green is also surrounded by three bunkers, one in the front and two behind the green, and a creek (Rae's Creek) just short of the green. The area on the sides of the front bunker is sloped towards the creek, and a garden and tall pine trees are present just beyond the far-side bunker. Thus, this hole is designed to severely punish inaccurate shots and this brings into the mix the final element: wind.

From the TMY3 (Typical Meteorological Year-3) weather data file of the nearby Augusta Bush Field Station (33.36°N, 81.96°W, and 40 m altitude), the average and maximum wind speeds during the first 2 weeks of April, when the tournament is held, are 2.9 and 8.8 m s^{-1}, respectively, with directions mostly between 200° and 250° from North. However, it is not just the wind speed, but the swirling wind patterns generated by the complex tree canopy (up to 30 meters high) around this hole that couple with the inherent difficulty of the hole to evoke uncertainty, and even fear among professional golfers [1, 2, 4, 5]. One common strategy among players is to take their shot at the 12th green when the flags on the 11th and 12th greens whip in a same direction. Given the variability of the wind, this is, however, not a common occurrence, even though these two greens are only 91 m (100 yd) apart [6]. Due to the wind-induced uncertainty, club selection for this hole can range from a 6- to a 9-iron during the tournament [7].

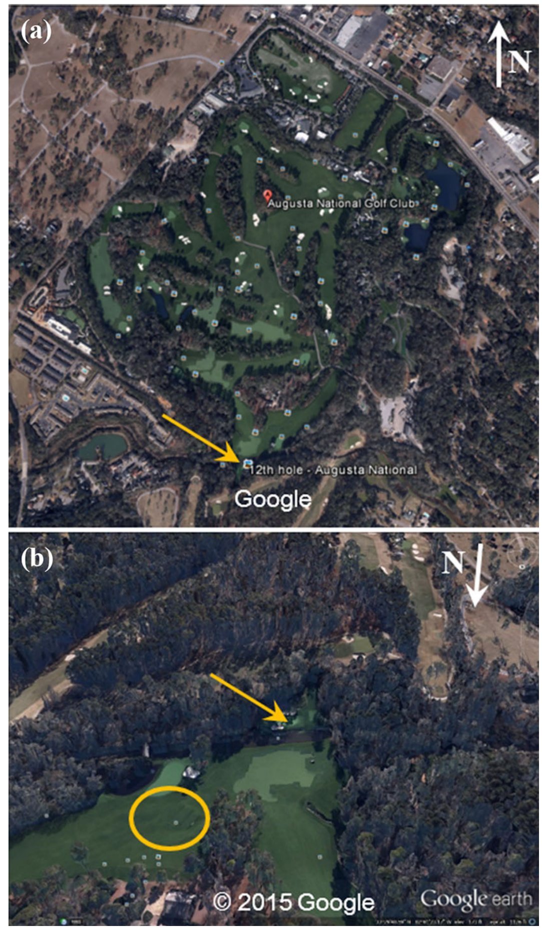

Fig. 1 Satellite view of **a** Augusta National Golf Club, and **b** south view of the hole 12 play area from 'Google earth'. The 12th green and its tee box are shown with an *arrow* and a *circle*, respectively

The wind-induced complexity of shot-making on this hole, therefore, makes this hole an ideal candidate for our analysis. In particular, we use computational modeling to determine the key wind-related factors that affect the accuracy of the shots at 12th hole as well as to understand the role that the local tree canopy plays in modifying the trajectory of the golf ball at this hole.

3 Model description and simulation setup

3.1 Golf ball motion and aerodynamic forces

The aerodynamics of golf balls and the effect of golf ball designs and swing on the ball flight and carry distance have been the subject of several past studies (e.g., [8–14]). Based on our current understanding of the motion of golf balls, the trajectory can be described by the Newton's second law of motion as follows:

$$M_{\mathrm{b}}\frac{\mathrm{d}\vec{U}_b}{\mathrm{d}t}=\vec{F}_{\mathrm{D}}+\vec{F}_{\mathrm{L}}+M_{\mathrm{b}}\vec{g}, \tag{1}$$

in which M_{b} is the golf ball mass, $\vec{U}_{\mathrm{b}}$ is the ball velocity, t is time, $\vec{g}$ is the gravitational acceleration, and $\vec{F}_{\mathrm{D}}$ and $\vec{F}_{\mathrm{L}}$ are the aerodynamic drag and lift forces, respectively (Fig. 2b).

Appropriate models are required to describe and parameterize the lift and drag forces on the golf ball. The drag force is assumed to be dominated by form drag that can be modeled in the standard way as follows:

$$\vec{F}_{\mathrm{D}}=-\frac{1}{2}C_{\mathrm{D}}\rho_{\mathrm{air}}A_{\mathrm{b}}\left|\vec{U}\right|\vec{U}, \tag{2}$$

where C_{D} is the drag coefficient and it is based on the empirical work of Bearman and Harvey [15], A_{b} is the projected area of the golf ball, ρ_{air} is the air density, and $\vec{U}\left(=\vec{U}_{\mathrm{b}}-\vec{U}_{\mathrm{w}}\right)$ is defined as the relative velocity of the ball and the local wind speed $\left(\vec{U}_{\mathrm{w}}\right)$. The lift on a golf ball is associated with the Magnus effect [16] that is generated due to the spin of the ball, this lift force can be modeled in the standard way as

$$\vec{F}_{\mathrm{L}}=\frac{1}{2}C_{\mathrm{L}}\rho_{\mathrm{air}}A_{\mathrm{b}}\left|\vec{U}\right|^{2}\frac{\left(\vec{\omega}\times\vec{U}\right)}{\left|\vec{\omega}\times\vec{U}\right|}, \tag{3}$$

where C_{L} is the lift coefficient and it is based on the empirical work of Bearman and Harvey [15], and $\vec{\omega}$ is the angular rate of spin imparted by the impact of the angled club-face on the ball.

Bearman and Harvey [15] have also shown that for the range of Reynolds numbers relevant for the flight of a golf ball, the lift and drag coefficients for golf balls are primarily functions of the spin parameter

$$S=(R|\vec{\omega}|)\Big/\left|\vec{U}\right|,$$

, which is the ratio of the surface velocity induced by the spin to the translational speed of the ball (with radius R). Bearman and Harvey [15] have also measured the lift and drag coefficients for a range of spin parameters ranging from about 0.02 to about 0.3, and this covers nearly the entire range of possible spin conditions for a typical golf shot. In the current study, we have digitized the experimental data of the lift and drag coefficients on the golf ball given by Bearman and Harvey [15] and used this directly in our computational model. Given the above modeling framework, Eq. (1) for the golf ball motion can be integrated in time numerically and we employ an explicit fifth-order Runge–Kutta scheme [17] for this time integration. The typical time-step size for this integration is about 0.005 s, which provides about 1245 time-steps over the typical flight of the ball for the par-3 hole that is examined in the current study.

The initial conditions for this time integration include the launch velocity $\left(\vec{U}_0, \mathrm{m/s}\right)$, launch angle ($\alpha$, °), and rate of spin ($\vec{\omega}$, RPM) (Fig. 2a). These depend on the club employed and also the way in which the club is swung by the golfer. In the current study, we employ launch conditions considered average for a PGA professional and data of these values are obtained from TrackMan website [18]. In all of our studies, the ball diameter and mass are chosen to be $2R=42.67$ mm and $M_{\mathrm{b}}=45.93$ g, respectively, and these conform to the United States Golf Association (USGA) rules.

As a first step, we have conducted a series of studies to assess the accuracy of the above golf trajectory model and these initial validation studies are carried out in quiescent wind conditions, i.e., $\vec{U}_{\mathrm{w}}=0$. The atmospheric conditions correspond to ρ_{air} for all our simulations which is equal to

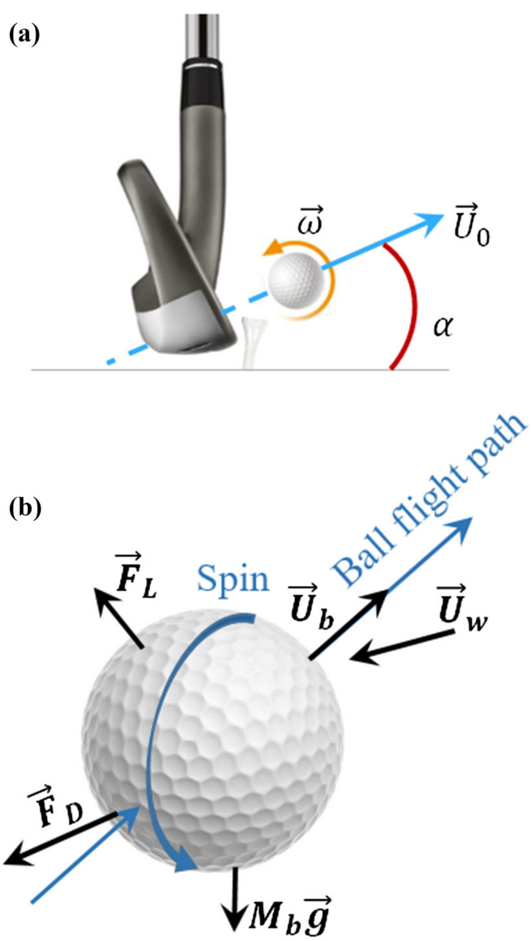

Fig. 2 **a** Schematic of launch velocity ($\vec{U}_0$, m s^{-1}), launch angle (α, °), and launch spin rate ($\vec{\omega}$, RPM); **b** schematic of the gravitational ($M_{\mathrm{b}}\vec{g}$) and aerodynamic drag ($\vec{F}_{\mathrm{D}}$) and lift ($\vec{F}_{\mathrm{L}}$) forces acting on a golf ball in flight

1.2 kg m^{-3}. The first comparison is to the results of Bearman and Harvey [15] for one particular case shown in their paper for which the launch conditions are as follows: launch velocity of 57.9 m s^{-1}, launch angle of 10°, and launch spin rate of 3500 rpm. Figure 3 shows a comparison of our predicted trajectory with that shown in Bearman and Harvey [15], and we note that the overall comparison is quite good. Although the current simulation predicts a slightly lower trajectory than Bearman and Harvey [15] (maximum difference is 8.5% of the maximum height), the carry distance is nearly identical. Potential sources for this difference can be errors in digitizing the Bearman and Harvey's results from their paper and/or the chosen value of the air density (1.2 kg m^{-3}) in our simulation that is not mentioned in Bearman and Harvey [15]. We also use our modeling procedure to predict the maximum height and carry distance of shots made with two different irons (7 and 9 irons), and these are compared to the PGA tour average [18] in Table 1. We note from the table that the results (calculated with air density of 1.2 kg m^{-3}) are in reasonable agreement with the PGA reference values with the carry distance and ball maximum heights showing maximum differences of about 3 and the 6%, respectively. The above comparisons show that the current modeling approach provides a good prediction of the key features of the trajectory of the golf ball for an average PGA professional.

3.2 Large-eddy simulation (LES)-based modeling of local wind conditions

The PArallelized Large-eddy simulation Model for Atmospheric and Oceanic Flows (PALM; Version 4.0) developed at the Institute of Meteorology and Climatology at Leibniz Universität Hannover [19] is used in the current work for simulating the flow field. PALM solves the non-hydrostatic, filtered, incompressible Boussinesq equations where the advection terms are discretized via Wicker–Skamarock-Scheme 5th-order scheme [20], and the time differencing is based on a third-order Runge–Kutta scheme [21]. To parameterize the subgrid-scale (SGS) covariance terms, following Deardorff [22], a prognostic equation is solved for the SGS turbulent kinetic energy (TKE) and surface momentum fluxes are parameterized using Monin–Obukhov similarity theory. A detailed description of PALM and its formulation can be found in Maronga et al. [23]. Compared to shear effects due to the very rough surface, buoyancy effects are considered to be of little importance here, and therefore, neglected.

The embedded canopy model of PALM is employed to model the volume averaged effects of plant canopies on the flow field in the domain. The plant canopy acts as a sink for momentum and its dynamical effect (C_{u_i}) depends on the vertical leaf area distribution (LAD), which is the leaf area per unit volume, the aerodynamic canopy drag coefficient (c_d), and the velocity components (u_i) [23]:

$$C_{u_i} = c_d \mathrm{LAD}\sqrt{u_i^2}u_i. \quad (4)$$

To accurately simulate the effects of the plant canopy on the flow field, vegetation topology around the 12th green is required to be input into the model. For this reason, PALM was modified to accept any plant canopy topology as an input binary file conforming to the Cartesian grid sets of the simulation domain. The exact (2D/top view) shape of the plant canopy topology around the 12th hole was found by applying the MATLAB image processing (Color Thresholder) tool on the 'Google Earth' image of the area of interest (Fig. 4).

From available images of the 12th hole scene in Augusta National Golf Club, it is estimated that the average height of the trees (denoted by H_c) surrounding this hole is around 15 times the height of the flagstick, or around 30 m. Similar to [24, 25], the canopy drag coefficient is assumed to be 0.2. The leaf area index (LAI), which is defined as the projected leaf area divided by the ground area, has typical values of 1–8 for sparse-to-dense canopies (e.g., [25–27]). The canopies around hole 12 appear to be dense and we, therefore, employ an LAI of 8. Following Markkanen et al. [25], Eq. (4) is defined based on the LAI multiplied by the beta probability density function with α and β coefficients of 5 and 3, respectively, that represent a canopy with a maximum foliage density located at the upper one-third of the canopy height (Fig. 1e of Markkanen et al.

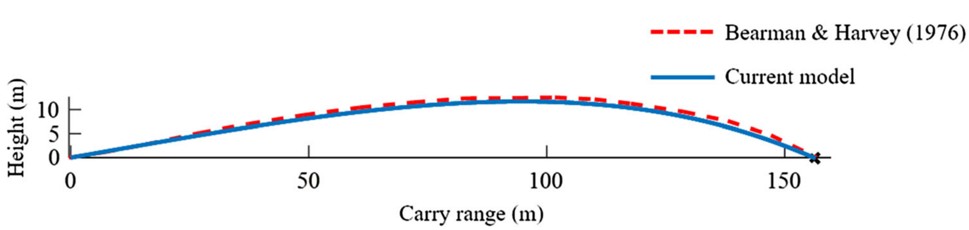

Fig. 3 Comparison of the modeled ball flight trajectory against the numerical model of Bearman and Harvey [15] for the launch velocity of 57.9 m s^{-1}, launch angle of 10°, and launch spin of 3500 rpm

Table 1 Comparison of the modeled and the PGA tour average [18] maximum flight height and carry range for 7 and 9 irons

	Launch speed (m s^{-1})	Launch angle (°)	Spin rate (rpm)	Maximum height (m)		Carry distance (m)	
				Current model	PGA tour average	Current model	PGA tour average
7 iron	53.6	16.3	7097	27.4	29.2	157.8	157.2
9 iron	48.7	20.4	8647	29.1	27.4	139.6	135.3

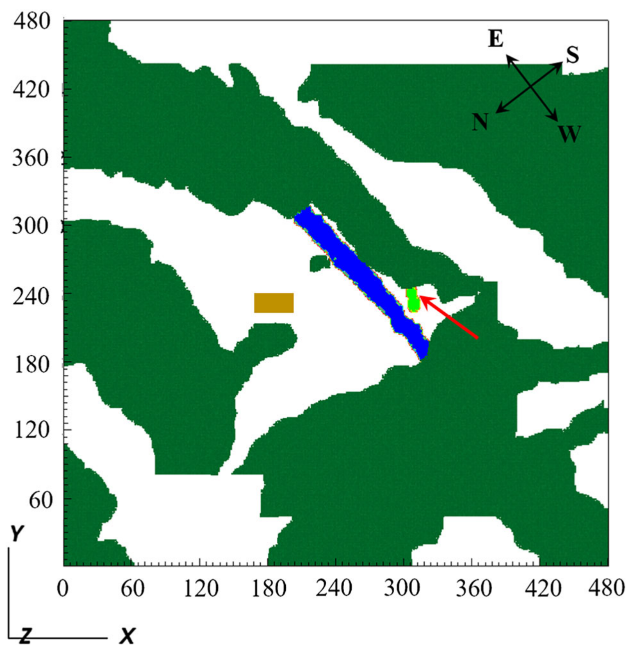

Fig. 4 Horizontal section (480 m × 480 m) of the simulation domain used in the LES with the 12th hole 142 m (155 yd) play area in the *middle*. Locations of trees, Rae's Creek, and the 12th green are shown in *dark green*, *blue*, and *light green* (and a *red arrow*) *shades*, respectively. Location of the 12th *tee box* is shown with a *brown color box* (color figure online)

[25]). It is assumed that the ground is flat at this location and the surface roughness length of the parts of ground not covered with the trees is taken to be 0.03 m, even though its effect on the turbulent flow is negligible compared to the effects of the plant canopies.

3.3 Simulation setup

The computational domain is cuboidal in shape with periodic boundary conditions on the horizontal boundaries. In the vertical direction, no-slip, non-penetration condition is applied on the lower boundary and free-slip boundary conditions are used on the top boundary. Given these boundary conditions, an appropriate size is needed for this computational domain. The chosen domain size should be large enough to include the largest eddies over the area of interest. The size of the largest eddy is determined by defining an integral length scale that is a measure of the largest correlation distance between two points in the turbulent flow [28]. This integral length scale is defined by the following:

$$L = \int_0^\infty R_{ii}(r,t)\mathrm{d}r \tag{5}$$

in which r is the spatial distance between two points in the flow and R_{ii} (r, t) is the longitudinal autocorrelation function for the stream-wise velocity component. In the horizontal plane, five different square domains with widths ranging from 2 to 4.5 times the length of the 12th hole (i.e. 155 yd), which contain the corresponding plant canopy topology in the area, were tested. The results indicated that energy containing eddies are about 42 m in size and a domain of 480 m × 480 m (around 3.4 times the length of the 12th hole) leads to results that are quite independent of the domain size. Note that this domain size is over 11 times the integral length scale and this is larger than the criteria (at least eight times) mentioned in Pope [29] for isotropic turbulence. Evidence of the influence of large coherent structures on the near-wall turbulent flow (e.g., [30–32]) necessitates an appropriate domain height to include the effect of these large-scale eddies that form within the inertial sub-layer (e.g., [33, 34]). According to Inagaki et al. [33], the inertial sub-layer for cube arrays of size H forms at heights between about 1.5H and 6H, and based on wind-tunnel experiments of Cheng and Castro [34], it forms between 1.8H and 2.4H. The domain height for our simulations was at least 20 times the canopy height to ensure that it contained the inertial sub-layer formed over the complex plant canopy topology in the domain. Figure 4 shows a horizontal cross section of the simulation domain, cut through the plant canopy height.

The grid employed in the horizontal directions has equal and uniform grid spacing. In the vertical direction, the grid spacing is uniform up to $z = 90$ m, which is three times the plant canopy height and gradually increases with an expansion ratio of 1.08 to the domain edge. To choose an appropriate grid resolution, flow simulations on the chosen domain were carried out with five different grids with nodal spacing of 0.5, 0.6, 1.0, 1.5, and 2.0 m in the horizontal and refined vertical domains, and the results of the flow field and the golf ball trajectory were examined. Figure 5 shows a sample

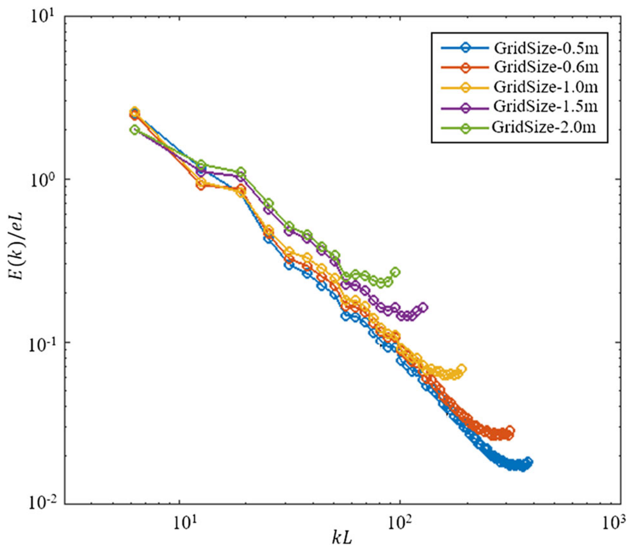

Fig. 5 Three-dimensional energy spectrum obtained from the velocity fields of the domain for five simulations with different grid sizes of 0.5, 0.6, 1.0, 1.5, and 2.0 m (color figure online)

three-dimensional (3D) energy spectrum [35] of the velocity field from the domains with five different grid sizes, and the convergence of the spectrum with grid size reduction shows that a grid resolution of 1 m provides an accurate representation of a wide range of spatial velocity scales. Results for the trajectory of the ball and its landing spot are nearly grid independent for this grid resolution. The overall grid size employed in these simulations was 480 × 480 × 144.

3.4 Simulations

A total of 32 separate simulations with wind speeds of 3, 6, 8, and 10 m s^{-1}, each with eight wind directions conforming to the eight principal geographical directions, were performed. Wind speeds were chosen to cover the range of average (2.9 m s^{-1}) and maximum (8.8 m s^{-1}) wind speeds based on the TMY3 weather data file of Augusta Bush Field (Sect. 2). Each simulation was performed over a time duration of 12 h and 10 instantaneous 3D velocity fields over the last 1200 s were stored for the calculation of golf ball trajectory. Ball trajectories are obtained for each of these 10 flow realizations and the resulting 10 distinct ball trajectories are then used to determine the variability of shot accuracy due to the wind. It is noted that the 120 s gap between each flow realization is significantly larger than the turnover time of the largest eddies in the flow (estimated to be about 14 s), ensuring the ball trajectories for a given wind condition 'sample' different large eddies in the flow. It is also noted that in the golf ball trajectory model, the wind velocity at the location of the ball in the air ($\overrightarrow{U}_{\mathrm{w}}$) was found through a linear interpolation between the velocities at the adjacent grid points to the golf ball coordinate in the flow field domain.

A more realistic golf ball trajectory simulation would use a temporally variable velocity field during the flight time (a coupled simulation) as opposed to the instantaneous, frozen velocity fields. To estimate the potential differences in these two situations, one case of golf ball trajectory simulation was performed using the temporally variable velocity field from the LES for the 8 m s^{-1} NW wind. Since the golf ball flight time for this wind is 7 s, seven instantaneous velocity fields with 1 s interval were used to do this dynamic field simulation. These velocity fields were used for temporal interpolations during the flight time.

For comparison, the landing spot found from the coupled simulation is compared against the landing spot of the mean trajectory of the seven trajectories each computed using seven subsequent instantaneous LES flow field outputs. The results indicate that the landing spots of the two cases are only 0.07 m apart, and the distance of the landing spot of this mean trajectory from the landing point of the no-wind case is only 0.05 m (or 0.8%) different than that of the coupled simulation. In addition, the standard deviation of the landing points of the seven instantaneous flow field-trajectories with respect to the landing point of the mean trajectory is 0.2 m, which is roughly an order of magnitude smaller than the typical standard deviation of this case. More accurate time integration techniques such as this can be employed for calculating the ball trajectory once the velocity field has been obtained, but this has implications for the computational complexity and data storage requirements of the trajectory calculation.

4 Results and discussion

For a professional golfer, in a calm, no-wind condition, 8- and 9-irons with an average carry distance of 146 m (160 yd) and 135 m (148 yd), respectively [18], are appropriate choices for a 142 m (155 yd) shot. In the current study, the 9-iron with a PGA tour average of 48.7 m s^{-1} launch speed, 20.4° launch angle, and 8647 rpm launch spin [18] was chosen for the golf ball trajectory simulations. The simulated flight trajectory of a 9-iron club for a no-wind case is shown in Fig. 6. The air density was 1.2 kg m^{-3} in all of the ball trajectory simulations that are representative of the altitude of the Augusta National Golf Club. The current model shows that with these launch conditions and no wind, the ball carries about 140 m (153 yd) and lands on the green. The launch point on the tee was fixed to this location for the rest of the study.

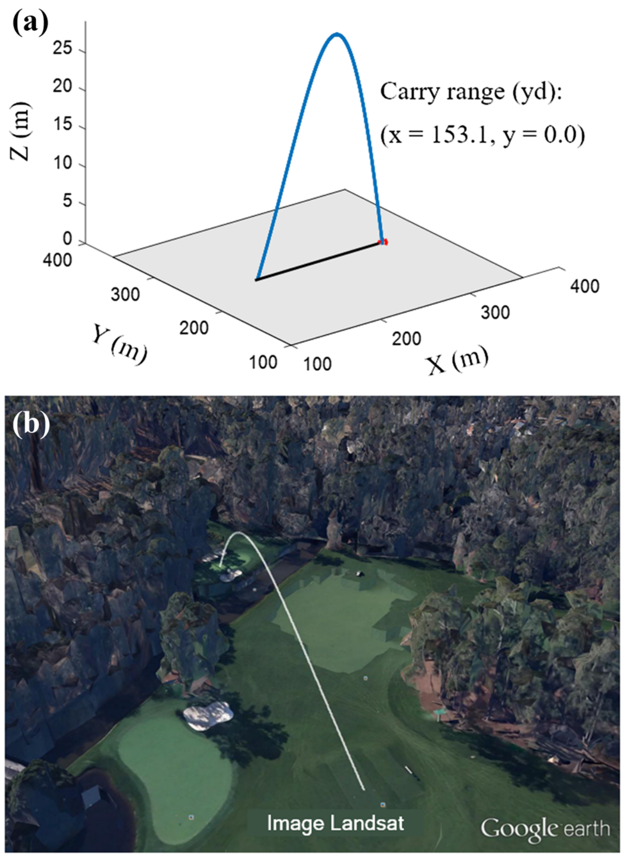

Fig. 6 Simulated golf ball flight trajectory using a 9-iron for a no-wind case **a** with respect to a 142 m (155 yd) distance, and **b** mapped over 'Google earth' image of hole 12 in Augusta National Golf Club

4.1 Flow patterns on hole 12

In this section, we examine the characteristics of the flow patterns around hole 12 to assess the possible effects of the plant canopy on the ball flight. Figure 7 shows the vortex structures generated by the canopy for one representative case that corresponds to a tail-wind (NE) at 6 m s^{-1}. The trajectory of the ball for the no-wind case is inserted into the plot and it can be observed that the entire path of the ball is within a zone that would be influenced by flow associated with the canopy. Thus, it is expected that for this hole, the plant canopy will play a significant role in determining the landing location of golf balls.

Figure 8 shows the variations in mean wind speed and velocity fluctuation variances on the plane of the ball flight trajectory for a variety of cases with wind speed of 8 m s^{-1}, and these demonstrate the potential effect that the combination of plant canopy and wind direction can have on the golf ball trajectory. Figure 8a compares the mean wind for the three cases: head (SW) wind with no canopy, headwind with canopy, and side (NW) wind with canopy. As can be seen, the average wind speed along the path of the ball is significantly affected by the presence of the canopy. The wind speed is generally higher for the no-canopy case and this is due to the presence of low-speed wakes that are created by the canopies. In the cases with canopy, the wind direction also has a significant impact on the distribution of the average wind speed due to the non-uniform distribution of the canopy around the ball flight path.

Figure 8b shows the corresponding plots for the mean velocity fluctuation variances and we note that the fluctuations are smaller for the no-canopy case and also depend noticeably on the wind direction for the with-canopy cases. The magnitude of these fluctuations will directly impact the variability in the ball trajectory as well as the landing spot of the ball and we, therefore, expect more unpredictability in the landing spot with the canopy. This issue is explored in detail in the next section.

4.2 Plant canopy effects on the accuracy of shots

Figure 9a shows sets of trajectories for the three selected wind conditions (SW, NW, and N 8 m s^{-1} winds), and

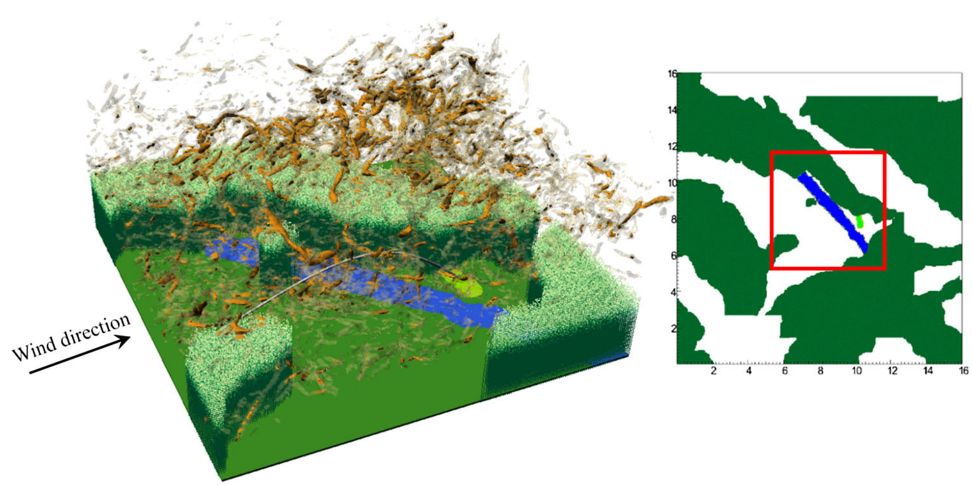

Fig. 7 Snapshot of simulated vorticity field from the center of the whole simulation domain for a 6 m s^{-1} NE wind. The *figure* shows iso-surfaces of vorticity that vary between 0.4 and 0.9 s^{-1}. The *white line* shows the trajectory of the ball for the no-wind case (color figure online)

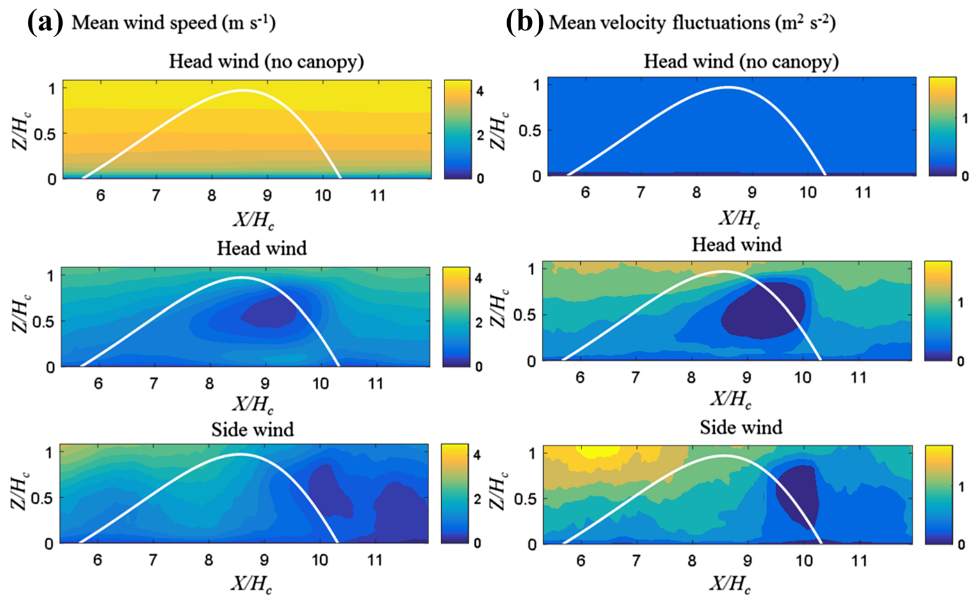

Fig. 8 Vertical cross sections of contours of the time averaged (over 1800 s) **a** wind speeds and **b** velocity fluctuation variances for the 8 m s^{-1} head (SW) wind with no canopy, headwind with canopy and side (NW) wind with canopy. The *white line* shows the golf ball trajectory simulated for a no-wind case, as a reference (color figure online)

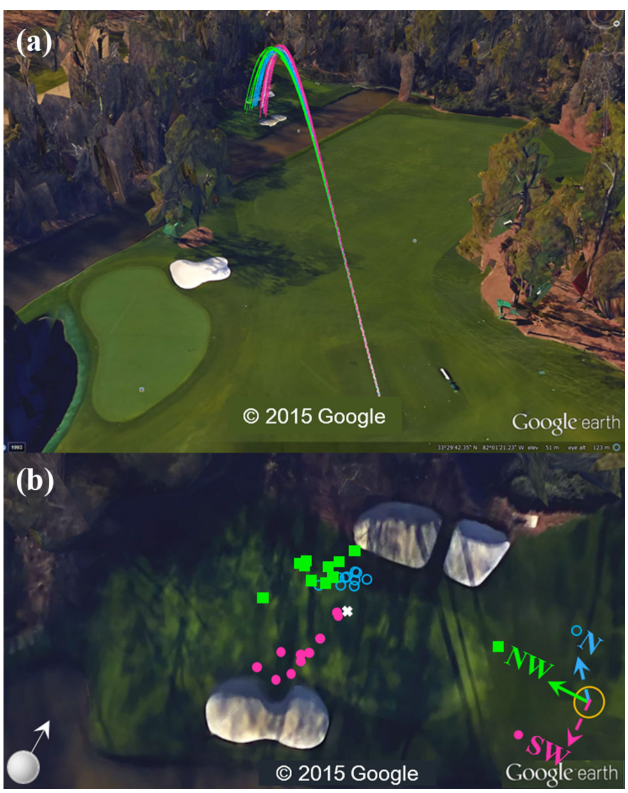

Fig. 9 **a** Simulated golf ball flight trajectories using a 9-iron club and **b** the ball landing spots for north, northwest, and southwest (head) 8 m s^{-1} winds, mapped on 'Google earth' images of hole 12 in Augusta National Golf Club. The *white color* flight trajectory and landing spot is related to the no-wind case (color figure online)

Fig. 9b shows the corresponding landing spots for these trajectories. It is clear that not only the average landing spot but the degree of deviation of the ball around this average spot depends significantly on the wind direction. Both the average location as well as the deviation provide a quantification of the effect of wind on the accuracy of the shot. Furthermore, since a key objective of the current paper is to explore the effect of the surrounding tree canopy on shot accuracy, we have also carried out the same set of 32 simulations (and corresponding ball trajectory calculations) with the tree canopy removed from the model. A comparison of these two situations allows for a delineation of the effects of the tree canopy on the difficulty of playing this hole.

4.2.1 Ball landing position

Figure 10 summarizes the computed data on the landing spot of the ball for all the cases simulated here for wind speeds of 3, 6, 8, and 10 m s^{-1}. The dark black lines in the polar plots denote the primary eight geographical wind directions and the direction of the ball flight is also shown in these figures with a small gray-colored circle. For each case, the statistics are based on the ten independent trajectory calculations each of which is based on the instantaneous 3D wind velocity field provided by the LES for that case.

Figure 10a, b compares the average golf ball landing spots (relative to the landing position of the ball in the no-wind case) for the various cases with and without the plant canopies, respectively. In the absence of the plant canopies and their wake flow, the mean wind and, therefore, the mean aerodynamic forces on a golf ball in flight are larger (not shown), and therefore, the distance of the average landing spot compared to the no-wind case is larger (over twice) than that of the cases with the plant canopies. For instance, at 6 m/s, which is a moderately high wind speed,

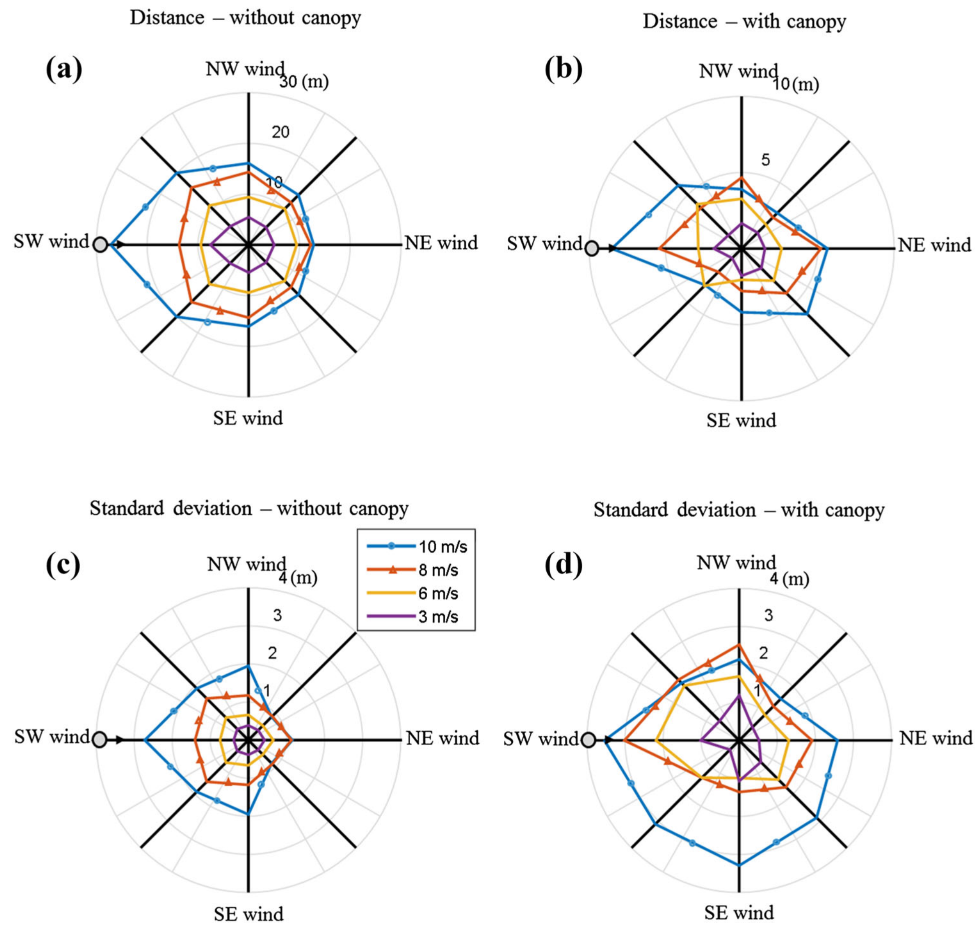

Fig. 10 Distance of the golf ball landing spot of mean trajectories with respect to the landing spot of the ball in a no-wind case for cases **a** without and **b** with plant canopies. Deviation range (m) of the golf ball landing position with respect to mean trajectories for different wind directions in cases **c** without and **d** with plant canopies (color figure online)

the landing spot with no canopy is about 10 m from the spot with no wind, whereas it is only between 2 and 3 m for the case with canopy. In addition, the average landing spot shows a well-defined distribution with wind direction for the no-canopy case; the distribution is symmetric about the ball flight path as expected and the headwind case showing the largest deficit (nearly 27 m) at the highest wind speed of 10 m s^{-1}. While the headwind case is also the one that shows the largest distance for the with-canopy case, the variation with wind direction is more complex, with crosswinds generating a smaller average distance to target. Thus, the presence of the canopy, while diminishing the overall effect of wind on the carry distance and landing spot, creates a more complicated variation of the landing spot with wind direction.

Another metric for evaluating the variability in the ball trajectory and landing spot due to the turbulent wind is the standard deviation (SD) of the ball landing position for each condition (wind direction and speed). The higher this standard deviation, the more difficult it would be for a golfer to predict the landing spot for a shot taken at any given instance in times for a given wind condition. Figure 10c, d shows this standard deviation in a polar plot for all the 32 wind conditions modeled here, without and with the plant canopy, respectively, and a number of observations can be made from these plots. First, the presence of the canopy produced a noticeably larger standard deviation in the landing position. For example, the SD for the 6 m s^{-1} SW headwind with canopy is over 2 m and this is nearly four times that for the same case without canopy. Second, the SD also shows a significant and complex dependence not only on the wind velocity but also the wind direction. Thus, for a golfer taking a shot at hole 12, the presence of the canopy clearly introduces a significant difficulty in predicting the landing spot for the ball in even moderately windy conditions.

5 Conclusions

In this study, a computational model has been developed to predict the effect of wind and local plant canopies on the trajectory of a golf ball on any particular hole of a golf course. A series of simulations were conducted to confirm the accuracy of the trajectory model under quiescent wind conditions. The model was then used to examine golf shots under different wind speeds and directions on hole 12 at the Augusta National Golf Club. The results from this model indicate that the golf ball flight path over hole 12 strongly depends on the combined effect of plant canopy topology and the wind direction. In general, a headwind on this hole creates the largest uncertainty in the landing spot of the ball. While the focus of the current research has been on one particular hole, the model could be applied to predict the effect of wind and plant canopy on any hole on any golf course for which wind and plant canopy information can be obtained. As such, this computational model might find use in the various aspects of the game of golf including as an aid for golfers as well as for enriching the technical discussion and coverage of this sport.

References

1. Woods T One of the hardest par-3s in the world; you don't know where the wind is coming from. www.Fatpat.Com/Software/Personal/Augusta/Hole12.htm
2. Nicklaus J Probably one of the most difficult wind-condition par-3s in all of Golf. Not a hard hole without the wind. www.Fatpat.Com/Software/Personal/Augusta/Hole12.htm
3. No. 12 Golden bell, masters. www.Augusta.Com/Masters/Coursetour/hole12. Accessed 15 Nov 2015
4. Nicklaus J The first time I played the hole was in 1959. I was with Roger McManus, a Good Amateur. Roger Hit first and flew the green with a 6-iron. I hit a 7-iron and didn't get halfway across Rae's Creek that was my introduction to the wind at the 12th. www.Golfdigest.Com/Story/Augusta-12th-Hole-Guy-Yocom
5. Player G My first experience at Augusta, Ben Hogan and Sam Snead were playing together. Hogan gets up and hits a 7-iron in the back trap. Snead looks in Hogan's bag and he gets up and hits an 8-iron in the water that was a terrible way for me to have my first look at the 12th. They are two of the greatest strikers of the Golf Ball who ever lived, and you have one in the water and one over the green. I said, 'man, there must be something to this hole,' and of course, over the years, you realize it's true. www.Golfdigest.Com/Story/Augusta-12th-Hole-Guy-Yocom
6. Yocom G (2012) Swirling down the drain. Last modified february 29, 2012. www.Golfdigest.Com/Story/Augusta-12th-Hole-Guy-Yocom. Accessed 29 Dec 2015
7. PGA Masters Tournament (2015). www.Pga.Com/Masters/Course/2015//Tour/12. Accessed 05 Oct 2015
8. Choi J, Jeon W, Choi H (2006) Mechanism of drag reduction by dimples on a sphere. Phys Fluids 18:041702
9. Beratlis N, Squires K, Balaras E (2012) Numerical investigation of magnus effect on dimpled spheres. J Turbul 13:1–15
10. Smith C, Beratlis N, Balaras E, Squires K, Tsunoda M (2010) Numerical investigation of the flow over a golf ball in the subcritical and supercritical regimes. Int J Heat Fluid Flow 31:262–273
11. Aoki K, Muto K, Okanaga H (2010) Aerodynamic characteristics and flow pattern of a golf ball with rotation. Procedia Eng 2:2431–2436
12. Seo S, Nam C, Han J, Hong C (2013) Drag reduction of a bluff body by Grooves laid out by design of experiment. J Fluids Eng 135:111202
13. Daemi N, Henning S, Gibert J, Yuya P, Ahmadi G (2016) On generalized rolling of golf balls considering an offset center of mass and rolling resistance: a study of putting. Sports Eng 19:35–46
14. Balzerson D, Banerjee J, McPhee J (2016) A three-dimensional forward dynamic model of the golf swing optimized for ball carry distance. Sports Eng 19:237–250
15. Bearman P, Harvey J (1976) Golf ball aerodynamics. Aeronaut Q 27:112–122
16. Mehta RD (1985) Aerodynamics of sports balls. Annu Rev Fluid Mech 17:151–189
17. Dormand JR, Prince PJ (1980) A family of embedded Runge-Kutta formulae. J Comput Appl Math 6:19–26
18. Trackman average tour stats, last modified June 6, 2014, Accessed October 7 2015. https://Blog.Trackmangolf.Com/Trackman-Average-Tour-Stats
19. PALM—a parallelized large-eddy simulation model for atmospheric and oceanic flows. https://palm.muk.uni-hannover.de/trac
20. Wicker LJ, Skamarock WC (2002) Time-splitting methods for elastic models using forward time schemes. Mon Weather Rev 130:2088–2097
21. Williamson J (1980) Low-storage runge-kutta schemes. J Comput Phys 35:48–56
22. Deardorff JW (1980) Stratocumulus-capped mixed layers derived from a three-dimensional model. Bound-Layer Meteorol 18:495–527
23. Maronga B, Gryschka M, Heinze R, Hoffmann F, Kanani-Sühring F, Keck M, Ketelsen K, Letzel MO, Sühring M, Raasch S (2015) The parallelized large-eddy simulation model (PALM) version 4.0 for atmospheric and oceanic flows: model formulation, recent developments, and future perspectives. Geosci Model Dev Discuss 8:1539–1637
24. Dupont S, Brunet Y (2008) Impact of forest edge shape on tree stability: a large-eddy simulation study. Forestry 81:299–315
25. Markkanen T, Rannik Ü, Marcolla B, Cescatti A, Vesala T (2003) Footprints and fetches for fluxes over forest canopies with varying structure and density. Bound-Layer Meteorol 106:437–459
26. Asner GP, Scurlock JM, Hicke JA (2003) Global synthesis of leaf area index observations: implications for ecological and remote sensing studies. Global Ecol Biogeogr 12:191–205
27. Cassiani M, Katul G, Albertson J (2008) The effects of canopy leaf area index on airflow across forest edges: large-eddy simulation and analytical results. Bound-Layer Meteorol 126:433–460
28. Hinze JO (1975) Turbulence, 2nd edn. McGraw-Hill, New York
29. Pope SB (2000) Turbulent flows. Cambridge University Press, Cambrigde
30. Hutchins N, Marusic I (2007) Large-scale influences in near-wall turbulence. Philos Trans A 365:647–664
31. Kanda M, Moriwaki R, Kasamatsu F (2004) Large-eddy simulation of turbulent organized structures within and above explicitly resolved cube arrays. Bound-Layer Meteorol 112:343–368
32. Perret L, Savory E (2013) Large-scale structures over a single street canyon immersed in an urban-type boundary layer. Bound-Layer Meteorol 148:111–131
33. Inagaki A, Castillo MCL, Yamashita Y, Kanda M, Takimoto H (2012) Large-eddy simulation of coherent flow structures within a cubical canopy. Bound-Layer Meteorol 142:207–222
34. Cheng H, Castro IP (2002) Near wall flow over urban-like roughness. Bound-Layer Meteorol 104:229–259
35. Davidson P (2015) Turbulence: an introduction for scientists and engineers. Oxford University Press, Oxford